

Maxwell's Thermal Creep in Two Space Dimensions

Koichiro SHIDA^{1,2,*} and Wm. G. HOOVER^{1,3}

¹*Department of Applied Science, University of California at Davis/Livermore,
Livermore, California 94551-7808*

²*Musashi Institute of Technology, 1-28-1 Tamazutsumi, Setagaya, Tokyo 158*

³*Lawrence Livermore National Laboratory, Livermore, California 94551-7808*

(Received January 14, 1998)

“Thermal Creep” is a steady streaming motion, induced by a temperature gradient parallel to a fluid boundary, in the absence of gravity. Thermal creep has been studied by Maxwell, analyzed by Kennard, and simulated by Ibsen, Soto, and Cordero. Here we report several two-dimensional simulations. We find that the creep velocity is sensitive to the imposed macroscopic boundary conditions and that the agreement with existing theoretical predictions is only semiquantitative.

KEYWORDS: statistical mechanics, molecular dynamics, kinetic theory, convection, converting heat to work

§1. Introduction

Maxwell explained thermal creep using ideas from kinetic theory.¹⁾ Consider a gas with a temperature gradient parallel to a confining wall. Because hotter particles impart more parallel momentum to the wall than do colder, a shear stress is exerted on the wall, with the gas flowing from colder to hotter as a reaction force. The resulting stationary velocity of the gas is the “thermal creep” velocity, and is parallel to the wall. The flow velocity is directly proportional to the temperature gradient. Ibsen, Soto, and Cordero reported computer simulations of thermal creep for two-dimensional hard-disk gases.^{2,3)} Though there were no gravitational forces, the flow patterns which they reported resemble the familiar convection rolls found in the Rayleigh-Bénard problem.⁴⁾ The reported maximum flow velocity, near the thermal walls, was found to be in excellent agreement with a “theoretical” thermal-creep-velocity value U_{\parallel} worked out in the same article:²⁾

$$U_{\parallel} = Q_{\parallel}/8P_{\perp\parallel}, \quad (1.1)$$

where Q_{\parallel} is the heat flux parallel to the wall, and $P_{\perp\parallel}$ is the pressure. We discuss the theoretical estimates further in §3.

Because this interesting problem is perhaps the simplest instance of converting heat directly to work, and also because the agreement with the theory was exceptionally good, we decided to extend these investigations, also in two dimensions, but using two different sorts of boundary conditions and four different system sizes. Our simulations, and our numerical results, are described in §2. Though in the main our results corroborate those of Ibsen, Soto, and Cordero, we find that the situation is a bit more complex than is suggested by the simple picture presented there. We find that the creep velocity depends not only on the heat flux but also on the boundary conditions. The “theoretical” estimate²⁾ is likewise

uncertain so that the agreement between simulation and “theory” is best described as semiquantitative.

§2. Simulations

Our simulations were carried out all at the same overall number density, N/V , and with the same hard-disk diameter, $\sigma = 0.2236$, as in ref. 2, so that the dimensionless density,

$$n\sigma^2 \equiv N\sigma^2/V = 1/20, \quad (2.1)$$

provided a collisional contribution to the pressure tensor of less than ten percent. The corresponding value of Maxwell's mean free path is $\lambda = 5\sqrt{2}\sigma = 1.58$. To save computer time, particles follow straight-line trajectories for a fixed timestep dt . If the distance between any pair of particles is less than σ , this pair needs to interact during the time step. In beginning our study we chose uniform random post-collision directions for the relative velocities of colliding particle pairs. The resulting simulations indicated the need for a more accurate treatment. The stochastic collisions eliminated velocity persistence (the statistically-averaged tendency of the particles to continue moving in their original direction after collision), and reduced the Prandtl number from four to two, modifying the higher moments of the velocity distribution unacceptably.⁵⁾ Accordingly, we repeated our work using exact post-elastic-collisional velocities for hard disk, interpolated to the precise time of each collision. There are two kind of boundaries. At an insulated boundary, hard-wall collisions occur whenever the separation between the wall and the center of a disk is less than $\sigma/2$. In treating thermal boundaries, particles hitting a thermostatted wall are ejected with a normal velocity drawn from the proper one-sided Gaussian distribution, $v_{\perp}f_{eq}$.

We chose a timestep:

$$dt \equiv 0.15\sigma(m/kT_H)^{1/2}. \quad (2.2)$$

The resulting heat flux between two parallel walls bounding a periodic channel was accurate to within five per-

* E-mail: shida@cs.musashi-tech.ac.jp

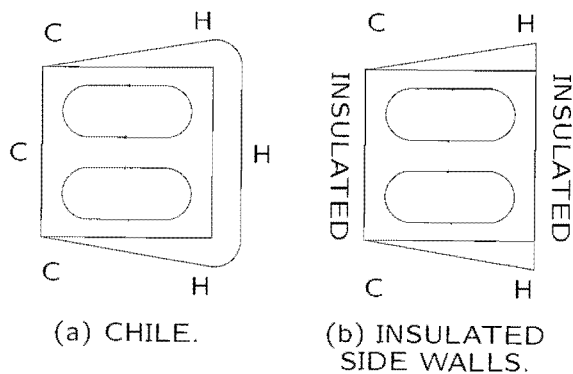


Fig. 1. Two-dimensional thermal creep geometry, “Chile” at the left, and “insulated” at the right. The insulated walls are perfectly reflecting. The width of the band on the thermostatted walls is proportional to the local wall temperature.

cent. For convenience we chose numerical values of Boltzmann’s constant k , the hard disk mass m , and the highest boundary temperature T_H all equal to unity. With a typical value of the timestep the mean distance covered by a high-temperature particle was about one-sixth the particle diameter. The finite time step reduces the effective collision rate by about one percent. A typical simulation consists of a quarter million hard-disk collisions, though results from much shorter runs are not really significantly different.

We employ the two system geometries shown in Fig. 1. The leftmost type, “Chile” geometry, is identical to that of ref. 2. The temperature difference between the cold left wall, at T_L , and the hot right wall, at T_H , causes uniform heat conduction. The top and bottom walls have a temperature gradient $\propto x^{-1/3}$, with the temperature continuous at the side walls. These boundaries cause thermal creep flow from left to right, parallel to the walls, returning to the left in the central region. The rightmost boundary type, “insulated”, has insulated side walls, so that the flow is only driven by the temperature gradient along the top and bottom walls.

Our computed temperature profiles along the top and bottom walls differ only very slightly from those of ref. 2. The temperature profile on the boundary $T \propto x^{2/3}$ corresponds to a constant heat flux with $\kappa \propto T^{1/2}$. This functional form does not allow for the existence of a temperature jump between the walls and gas near. Typical time-averaged flow and heat fields are shown in Fig. 2, for the Chile boundary conditions 2500 particles, with $V = L^2 = 20N\sigma^2$ and $T_H/T_L = 10$. Heat flows, roughly, parallel to the top and bottom walls. The mass flow forms two rolls, with the upper clockwise, and the lower counterclockwise. Figure 3 corresponds to the insulated geometry. Here the heat flux is very different because it is necessarily parallel to the vertical walls. Nevertheless, the mass flux is nearly identical to the Chile boundary conditions. The mass flux is smoothed, by using a weighting function,

$$w(x \equiv r/a) = (5/\pi a^2)(1-x)^3(1+3x), \quad (2.3)$$

where $a = 2(V/N)^{1/2}$, computing the mean velocity at grid points with a spacing equal to $a/2$. The fields are

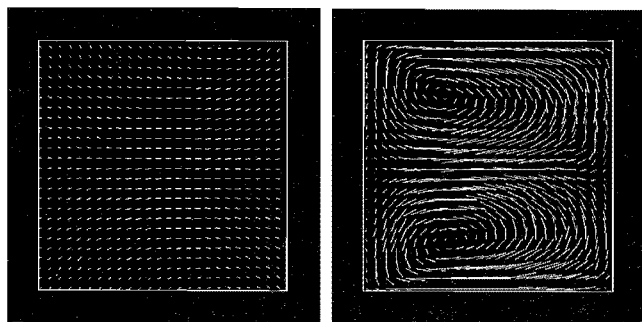


Fig. 2. Heat flux (left) and flow velocity (right) for $N = 2500$ particles with “Chile” boundary conditions. The temperature ratio for the two vertical walls is $T_H/T_L = 10$. The maximum heat flux is about 0.08 at the center and mean heat flux from right to left is 0.056. The maximum local creep velocity is 0.025. One fourth of all grid points are shown.

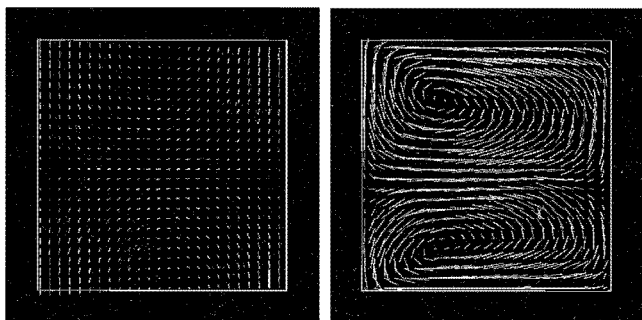


Fig. 3. Heat flux (left) and flow velocity (right) for $N = 2500$ particles with “insulated” boundary conditions. The maximum heat flux is 0.18 near the right wall and mean heat flux from right to left is 0.024. The maximum local creep velocity is 0.03. The length of vector is comparable with Fig. 2.

averaged over the final half of each simulation.

We follow the methods of ref. 2 to observe the creep velocity. First, we choose two rows in which the flow speed reaches the maximum values along each of the top and the bottom walls. The row is between second and fourth adjacent rows from the walls instead of the next. The velocity decrease near the wall is discussed in §3. Secondly, for example, central 28 points out of 38 are averaged for the creep velocity for 1444 particle case to avoid the effect of vertical walls. These parameters have been appropriately modified according to system size. This procedure provides two estimates of the creep velocity.

The ratio of the creep velocity to the thermal velocity at the hot wall is shown in Fig. 4 as a function of the inverse system length, measured in Maxwell free paths, λ/L . The creep velocity is a little higher in insulated geometry than Chile despite the smaller heat flux Q_{\parallel} . The nearly constant creep velocity, U for any system size is the result of two offsetting effects, the change of temperature gradient dT/dx with system size, and the intrinsic size dependence of the creep velocity. Roll rotation is promoted in larger systems by reduced viscous stresses.

§3. Comparison with Theoretical Estimates

One “theoretical” creep velocity¹⁾ pictures the velocity distribution function f near a thermostatted wall as the

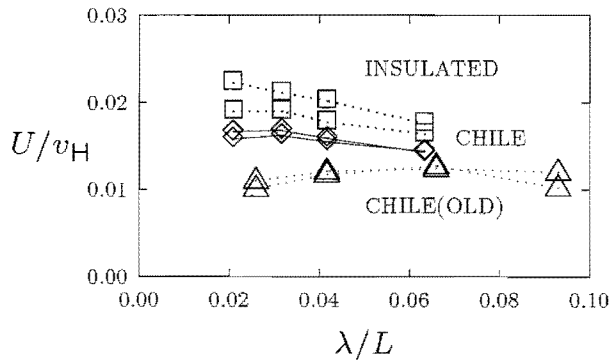


Fig. 4. Dependence of reduced creep velocity, U/v_H , on system size for both "Chile" and "insulated" boundary conditions. Each simulation gives two points, corresponding to the velocities near the top and bottom walls. The corresponding particle number for the four data sets are 625, 1444, 2500, and 5776. Data from ref. 2, as well as additional data furnished by its authors, are shown as triangles and labelled "Chile (old)".

average of a velocity distribution perturbed by dT/dx for incoming particles, and typical of the wall for outgoing particles:

$$f(v_{\perp} > 0) = f_{\text{equilibrium}}; \quad (3.1)$$

$$f(v_{\perp} < 0) = f_{\text{equilibrium}} \times \left\{ 1 + \tau v_{\parallel} \frac{d \ln T}{dx} \left[\frac{mv^2}{2kT} - \frac{D+2}{2} \right] \right\}, \quad (3.2)$$

in D dimensions. The collision time τ is

$$(15/32) \sqrt{m/\pi kT} / (n\sigma^2), \quad (3.3)$$

in three dimensions and $\sqrt{m/\pi kT} / (n\sigma)$ in two. The resulting mean shear stress at the wall, $\langle \rho v_{\perp} v_{\parallel} \rangle$, has the same value in both two and three dimensions:

$$P_{\perp \parallel} = (k/\sqrt{2}\pi\sigma)(dT/dx). \quad (3.4)$$

The assumption that this shear stress at the wall is exactly offset by a flow of parallel momentum from a uniform current parallel to the wall gives a creep velocity which can be expressed in terms of the gas-phase heat flux Q_{\parallel} :

$$U_{\parallel} = Q_{\parallel} / (D+2)P_{\perp \parallel}, \quad (3.5)$$

where D is again the dimensionality. This estimate is twice that of ref. 2, which uses a slightly different argument in relating the flow velocity to the shear stress. They assumed that the hydrodynamic velocity goes to zero exponentially with the distance to the wall, proportional to $\exp(-x/\lambda)$.³⁾ This is not in accord with the observed velocity profile shown in Fig. 5 in which U_{\parallel} reaches a maximum at about one λ away from the walls.

Our simulation suggest that the ratio of the creep velocity U_{\parallel} to the estimates varies about 0.8 power of the system width, and have no large-system size limit. See Fig. 6. Hence thermal creep is in fact more sensitive to the boundary conditions than to the heat flux. We observe the decrease in creep velocity near the walls predicted by Sone.⁶⁾ See Fig. 5 again. The decrease is due to molecules hitting the walls with a mean parallel ther-

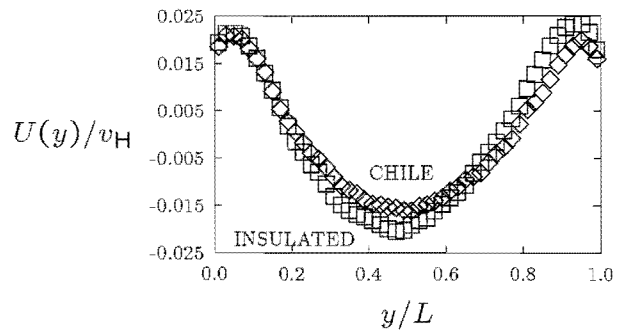


Fig. 5. Typical creep velocity distribution at $x = L/2$. U_{\parallel}/v_H reaches a maximum at about one λ away from the walls, and decreases nearer the walls. See ref. 5.

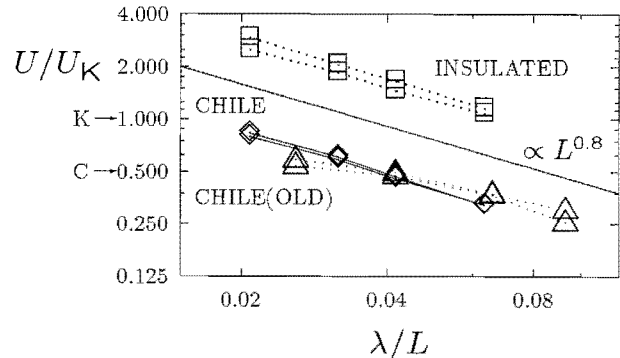


Fig. 6. Dependence of reduced creep velocity, U/U_K , where U_K is Kennard's estimate, on system size for both "Chile" and "insulated" boundary conditions. Heat flux Q_{\parallel} and pressure $P_{\perp \parallel}$ on which the estimate based are overall average of the systems. The "theoretical" estimate from ref. 2 is also shown, as U_C . Data from ref. 2, as well as additional data furnished by its authors, are shown as triangles. The reference line represents 0.8 power of the system width.

mal velocity opposite to the mass velocity. According to Sone's three-dimensional analysis, the velocity should increase from about thirty percent of the creep velocity at the wall, to the maximum creep-velocity value, at a distance of the order of a few Maxwell free paths. The velocity decrease found near the wall is slightly reduced by the averaging inherent in our smooth weighting function.

§4. Conclusion

Only a rough explanation of thermal creep was available to Maxwell. Our present understanding is not much better, and remains only semiquantitative. The simulations presented here reveal two kinds of dependency. There is a significant dependence of the results on system size because the roll size influences the viscous stresses. There is also a strong dependence on boundary conditions, which are necessarily idealized in any simulation. Comparing Figs. 4 and 5 suggests, as is quite plausible, that the second moment of the velocity distribution is a better reduction parameter for creep velocity than is the third, Q_{\parallel} .

Acknowledgements

A part of this work was performed at the Lawrence

Livermore National Laboratory, under the auspices of the United States Department of Energy through University of California Contract W-7405-Eng-48 and with the support of the Accelerated Strategic and Advanced Scientific Computing Initiatives. We thank Prof. Cordero and Dr. Soto, at the University of Chile (Santiago) for helpful discussions as well as for providing the unpublished data shown in the Figures, and further details of their simulation technique.

-
- 1) E. H. Kennard: *Kinetic Theory* (McGraw-Hill, New York, 1938).
 - 2) J. Ibsen, R. Soto and P. Cordero: *Phys. Rev. E* **52** (1995) 4533.
 - 3) P. Cordero and D. Risso: *Fourth Granada Lectures in Computational Physics*, ed. P. L. Garrido and J. Marro (Springer-Verlag, Heidelberg, 1997).
 - 4) V. M. Castillo, Wm. G. Hoover and C. G. Hoover: *Phys. Rev. E* **55** (1997) 5546.
 - 5) Wm. G. Hoover: *Computational Statistical Mechanics* (Elsevier, Amsterdam, 1991) p. 234.
 - 6) Y. Sone: *J. Phys. Soc. Jpn.* **21** (1966) 1836.
-